The Formation of Filament Threads in a Sheared Magnetic Field

Lawrence Sparks

Jet Propulsion Laboratory

Solar Activity During the Onset of Solar Cycle 24

Napa, California

December 10, 2008

Outline

- Why am I here?
- Thermal instability
- Condensation in a sheared magnetic field
- Linear analysis
- Nonlinear simulation

Observations

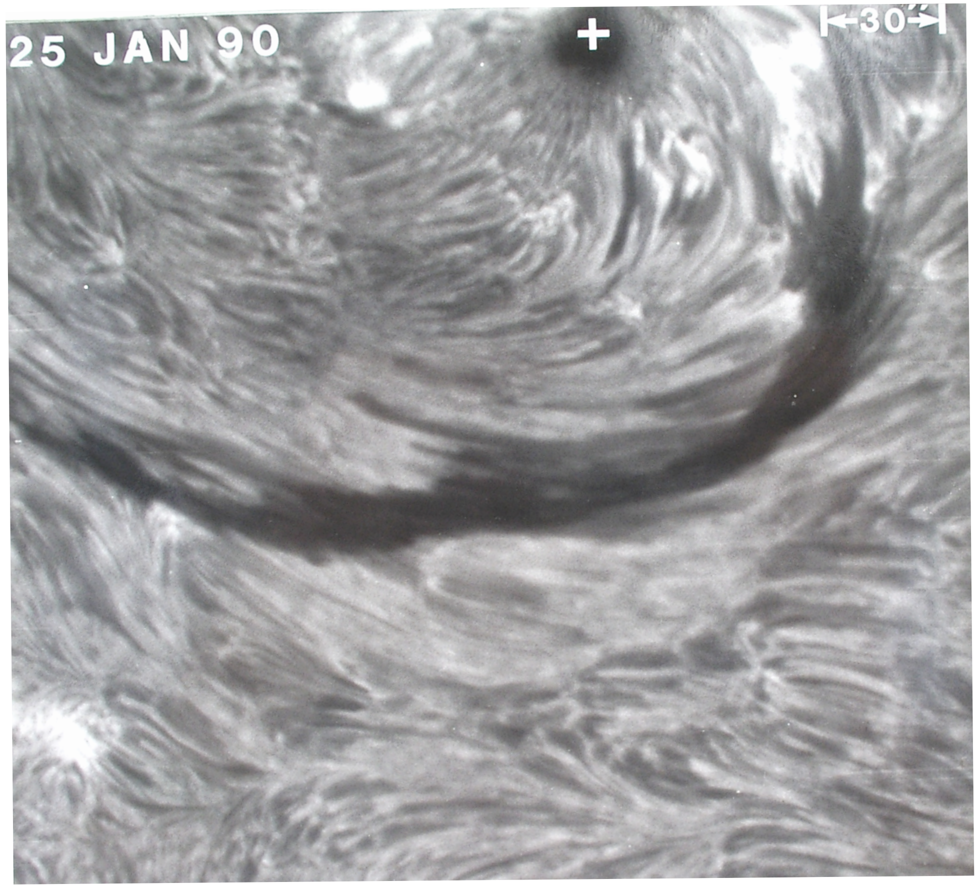

shown by Sara Martin at JPL Space Plasma Physics Journal Club, 8/22/2008

Filaments are observed to separate regions of opposite, line-of-site magnetic polarity in the photosphere.

Spectrum of filaments

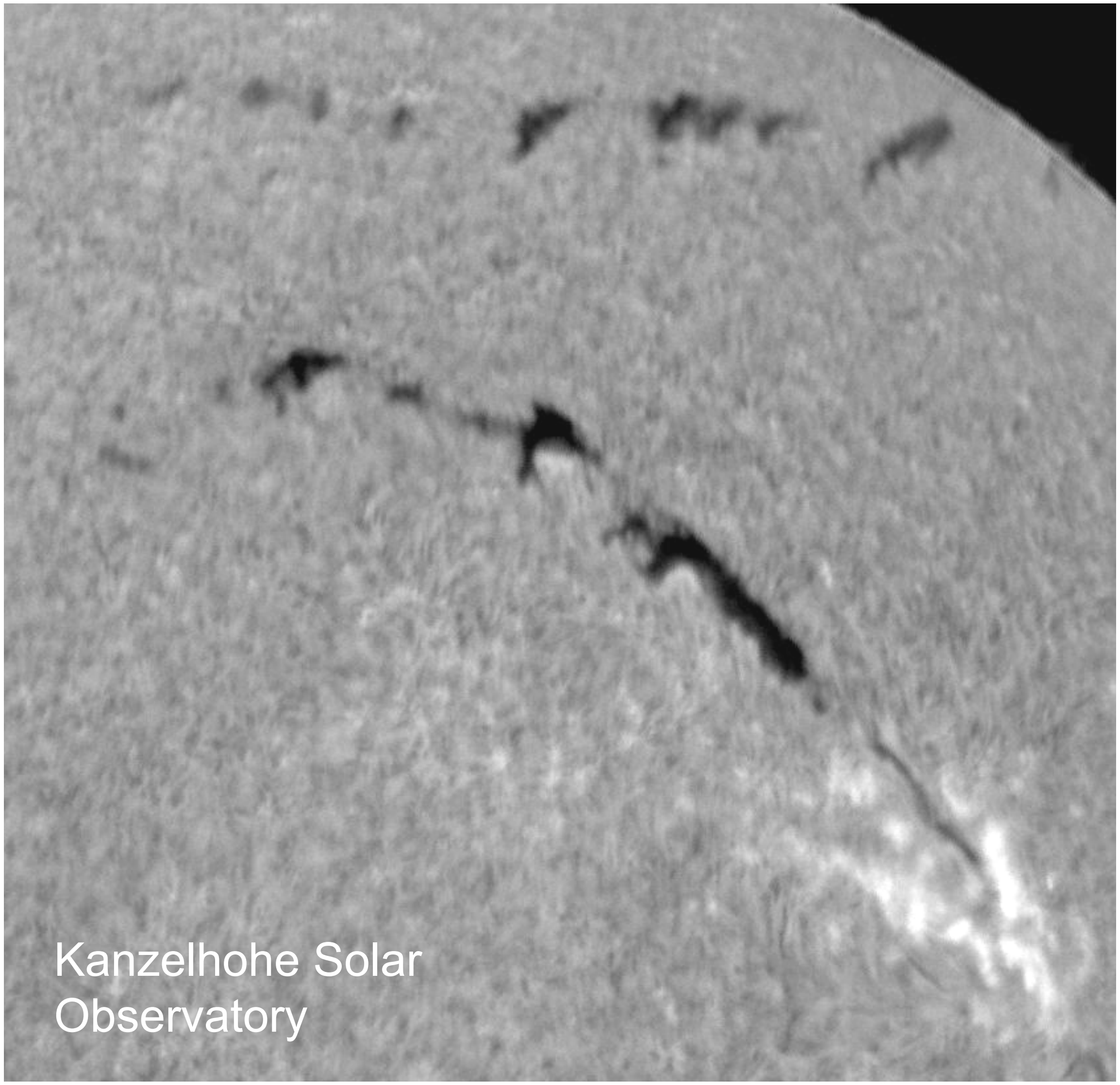

Quiescent polar crown filament

Quiescent filament

Intermediate filament

Active region filament

Magnetic field configuration for filaments (from Sara Martin)

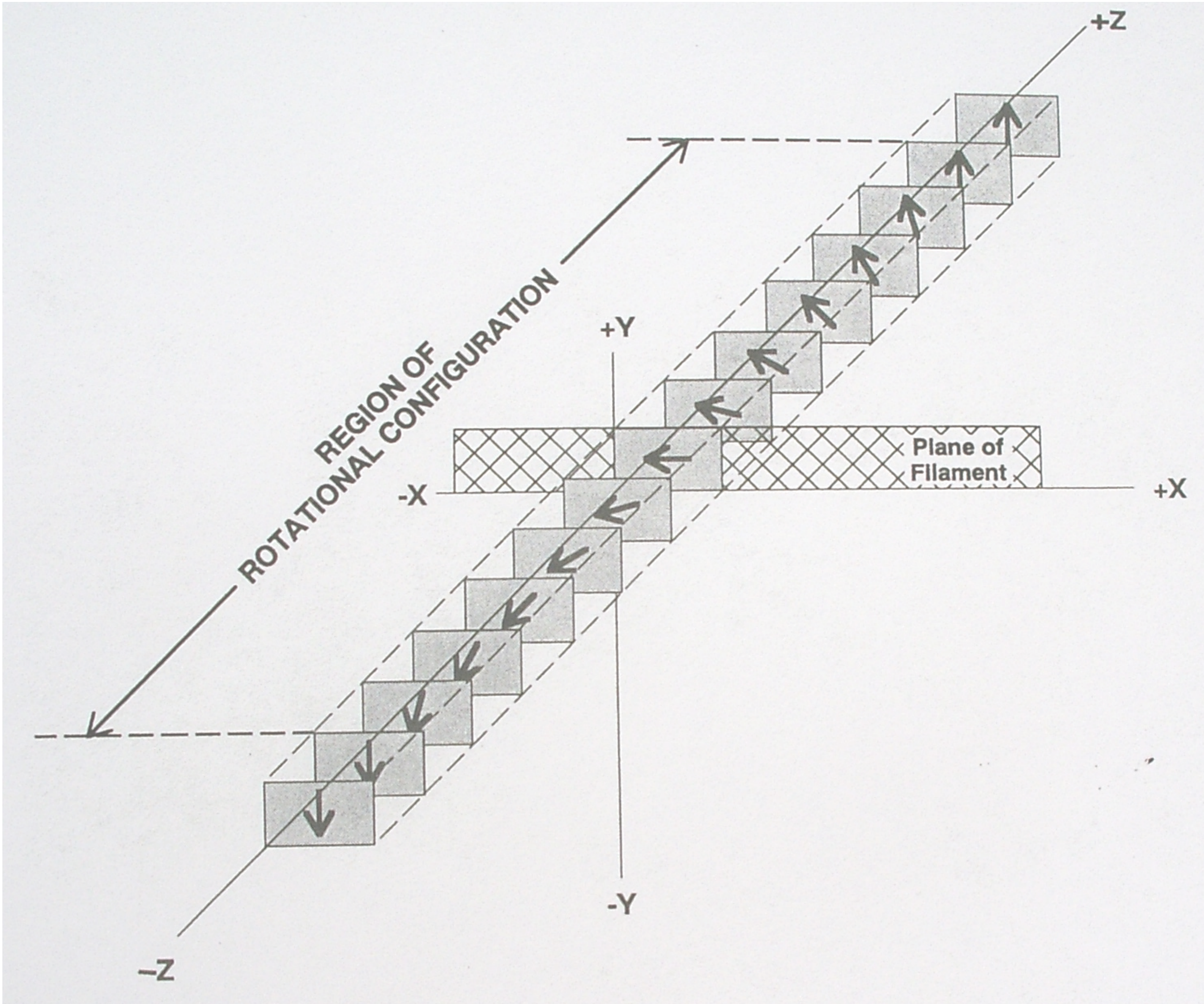

References on thermal instability in a sheared magnetic field

L. Sparks and G. Van Hoven, "Thermal Instability of a Radiative and Resistive Coronal Plasma", **Astrophys. J. 333**, 953 (1988).

L. Sparks, G. Van Hoven and D. D. Schnack, "The Nonlinear Evolution of Magnetized Solar Filaments", **Astrophys. J. 353**, 297 (1990).

Thermal stability

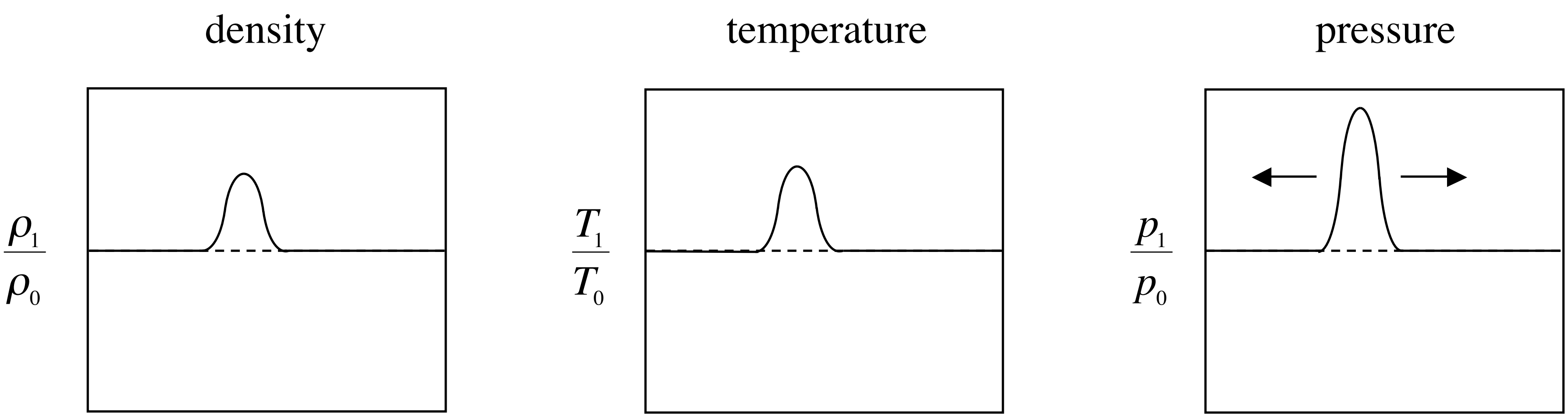

Adiabatic compression: perturbed pressure provides a restoring force

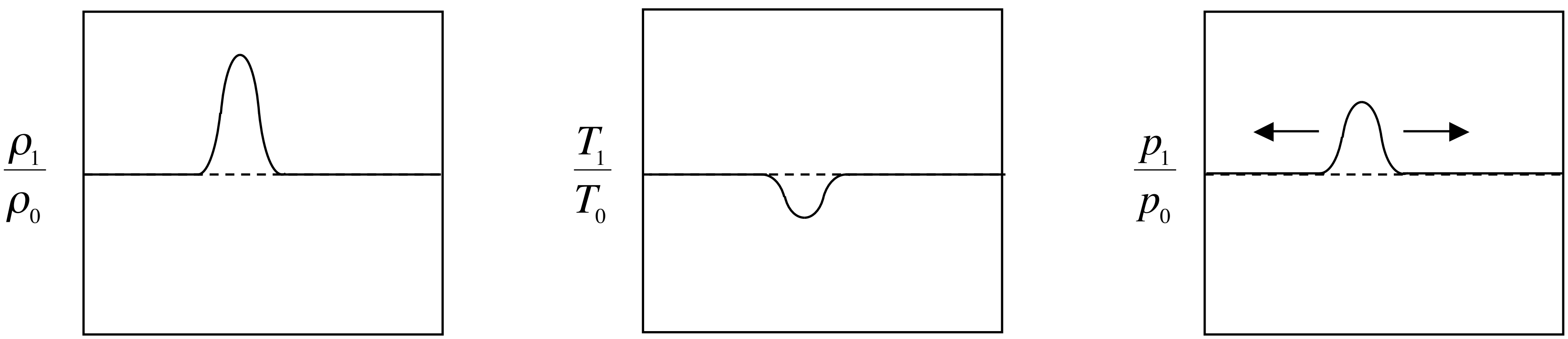

Thermal equilibrium with radiation: $H + C = 0$ $H = H(\rho)$ $C = R\rho^2 T^r$

Radiative compression: here adiabatic and non-adiabatic heating dominates

Thermal instability under coronal conditions

Temperature drop causes enhanced radiative losses.

Condensation augments radiative losses.

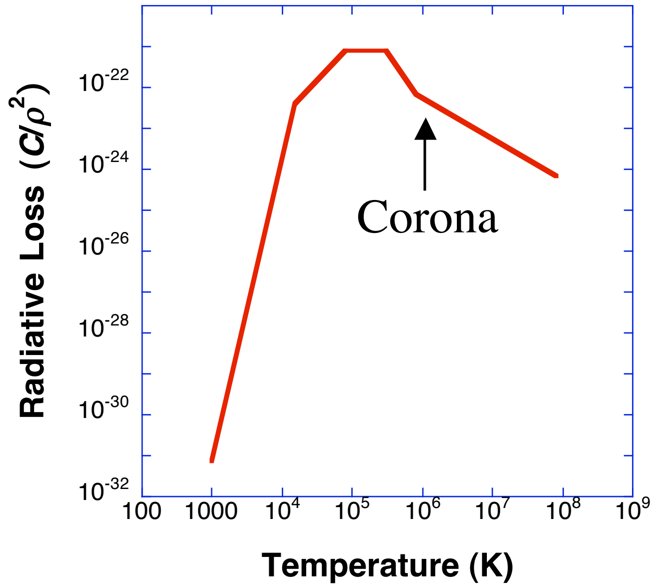

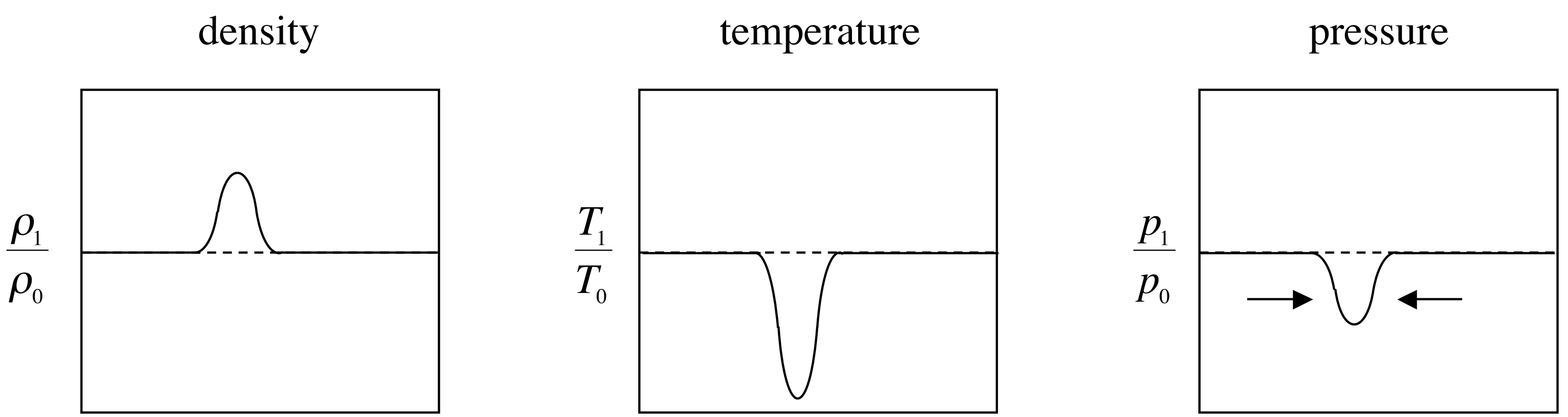

Thermal conduction

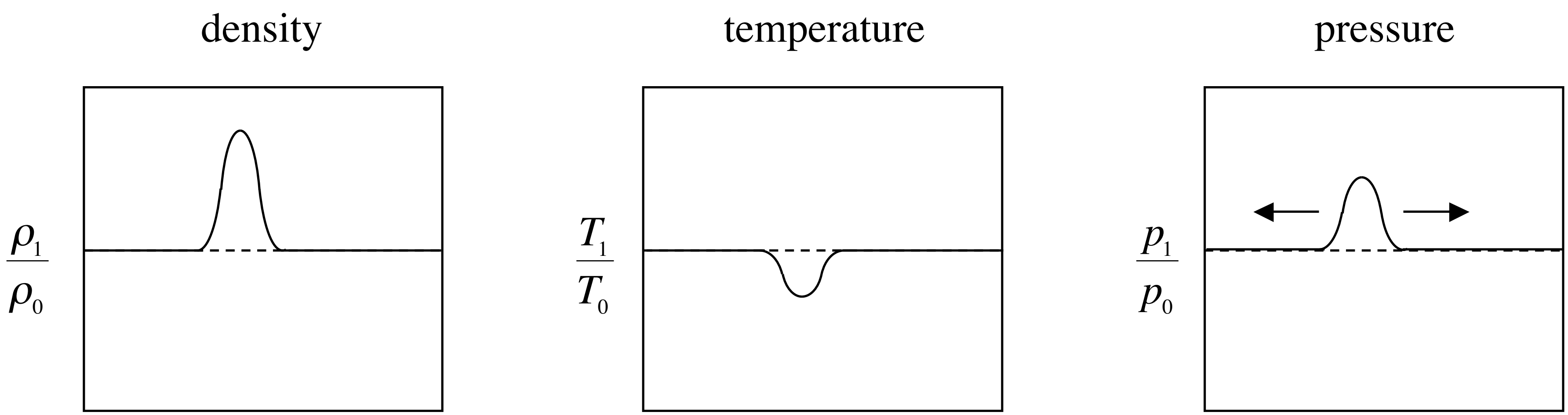

Compression with thermal conduction: heat flow stabilizes perturbation

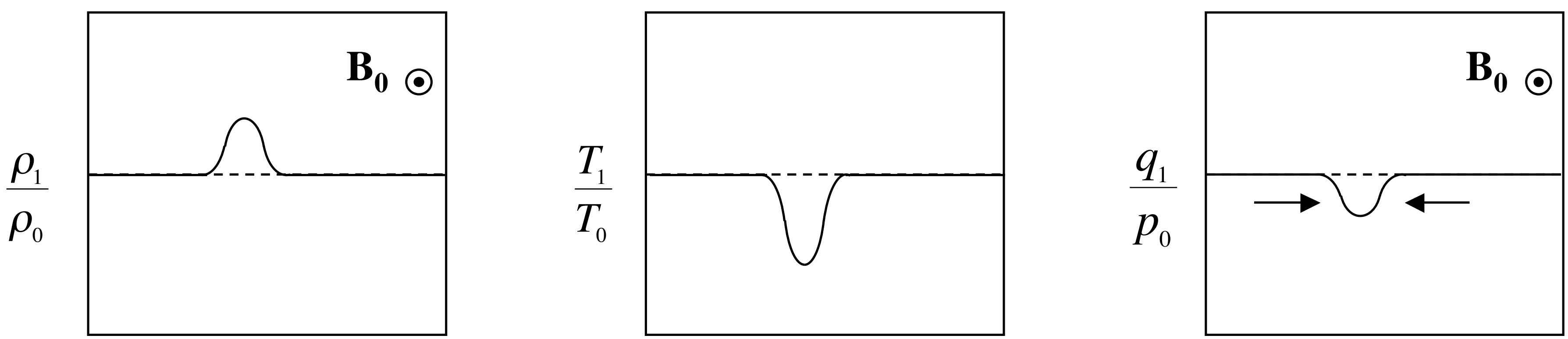

Compression with magnetic field: field provides thermal insulation in transverse direction
Magnetic pressure opposes density enhancement

Filament thread formation by condensational instability?

Condensational instability cannot form filament threads in a *uniform* magnetic field:

(1) the magnetic field prevents transverse mass flow from contributing to a local growth in density;

(2) heat flow parallel to the field ensures that parallel mass flow will not contribute to a condensational instability.

Key question:

How is it possible for a magnetic field to inhibit heat flow in a coronal plasma without simultaneously restricting the mass flow required for the growth of filament threads?

Condensations in a sheared magnetic field

Model equilibrium field

Perturbation
wave vector

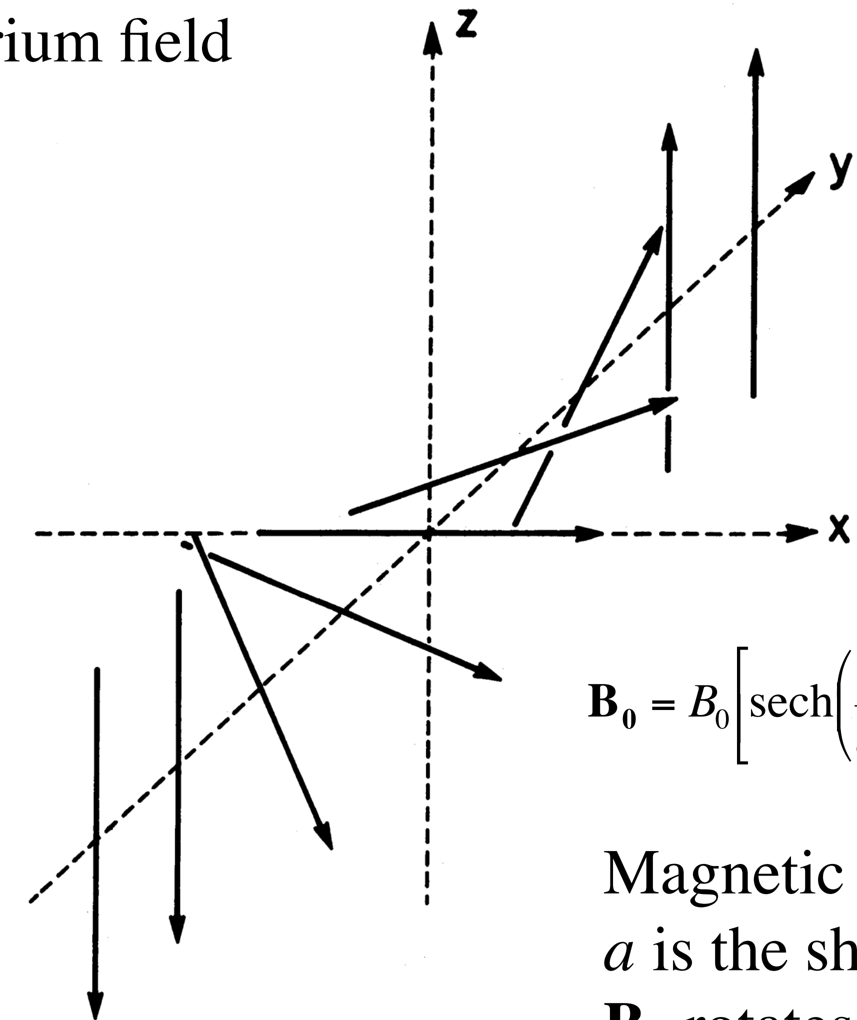

$$\mathbf{B_0} = B_0\left[\operatorname{sech}\left(\frac{y}{a}\right)\hat{\mathbf{e}}_\mathbf{x} + \tanh\left(\frac{y}{a}\right)\hat{\mathbf{e}}_z\right]$$

Magnetic field is force-free.
a is the shear scale.
$\mathbf{B_0}$ rotates 50˚ over [0, a].

Localization of density in the shear layer

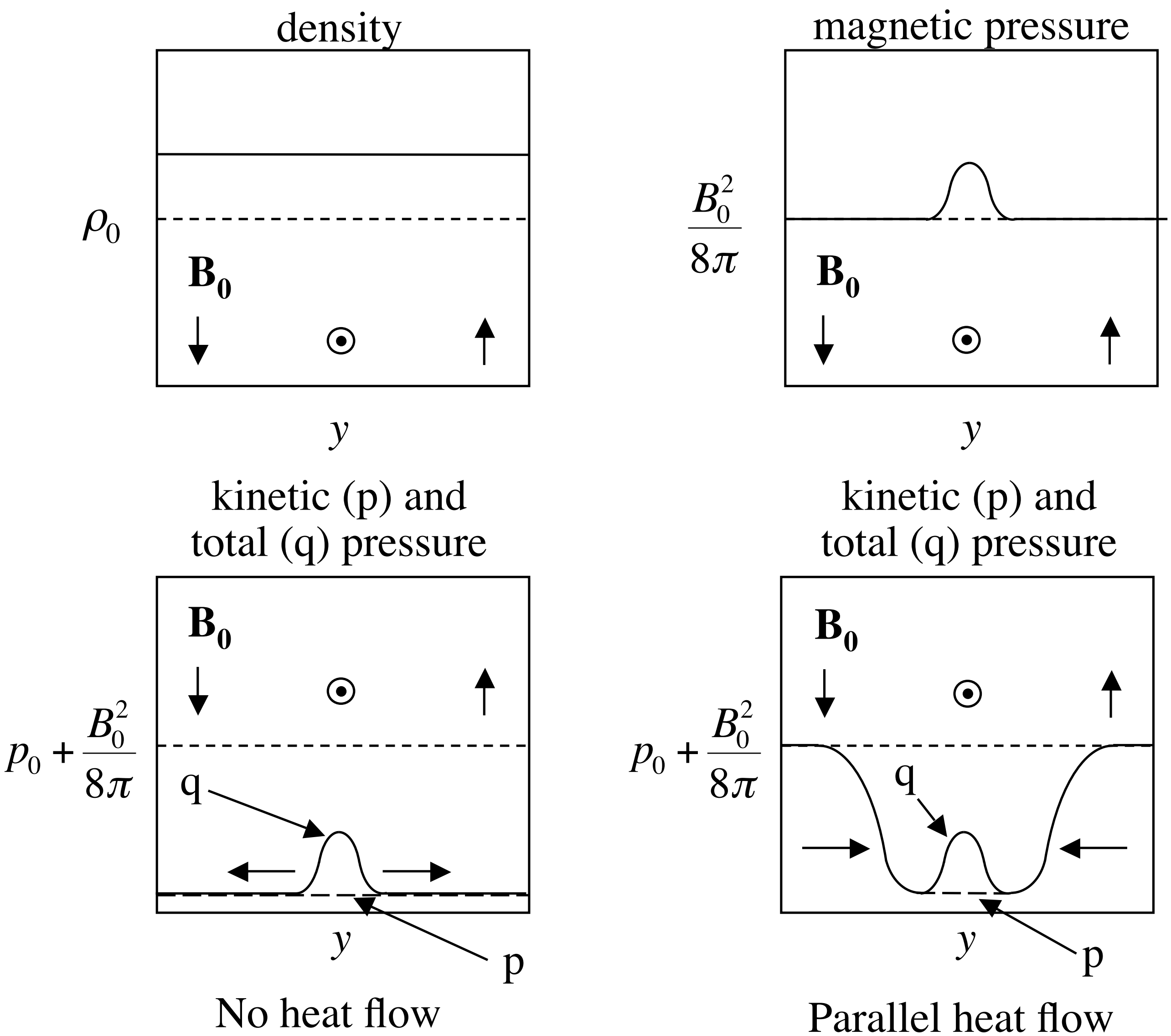

Parallel heat flow forces perturbation to vanish at boundary.

Total pressure gradient pushes plasma into the shear layer.

Model equations

Continuity eq.

$$\frac{\partial \rho}{\partial t} + \boldsymbol{u} \cdot \nabla \rho + \rho \nabla \cdot \boldsymbol{u} = 0 ,$$

Momentum eq.

$$\rho \left(\frac{\partial \boldsymbol{u}}{\partial t} + \boldsymbol{u} \cdot \nabla \boldsymbol{u} \right) + \nabla p - \frac{1}{c} \boldsymbol{J} \times \boldsymbol{B} = 0 ,$$

Maxwell's eqs.

$$\frac{1}{c} \frac{\partial \boldsymbol{B}}{\partial t} + \nabla \times \boldsymbol{E} = 0 , \qquad \nabla \times \boldsymbol{B} = \frac{4\pi}{c} \boldsymbol{J} ,$$

$$\nabla \cdot \boldsymbol{B} = 0 , \qquad \boldsymbol{E} + \frac{1}{c} \boldsymbol{u} \times \boldsymbol{B} = \eta \boldsymbol{J} ,$$

Assume classical (small) resistivity.
Note: no gravity.

Energetics

Ideal gas law

$$p = 2\rho k_{\mathrm{B}} T/m_i$$

Energy eq.

$$\frac{\partial p}{\partial t} + \boldsymbol{u} \cdot \nabla p = \frac{\gamma p}{\rho}\left(\frac{\partial \rho}{\partial t} + \boldsymbol{u} \cdot \nabla \rho\right) + (\gamma - 1)(\eta J^2 + H - C + \nabla \cdot \underset{\sim}{\boldsymbol{\kappa}} \cdot \nabla T)$$

Heating function *H* is assumed constant in time.

Classical thermal conductivity tensor **κ** has $\kappa_{\perp} << \kappa_{||}$.

Characteristic time scales

TABLE 1

CHARACTERISTIC CORONAL FREQUENCIES

Frequency	Definition	Value ($\Omega\tau_h$)
Ω_ρ	$-(\gamma-1)\left(\frac{T_0}{p_0}\right)\left(\frac{\partial C}{\partial T}\Big\vert_\rho\right)_0$	7.32×10^{-5}
Ω_T	$(\gamma-1)\left(\frac{\rho_0}{p_0}\right)\left(\frac{\partial C}{\partial \rho}\Big\vert_T\right)_0$	1.46×10^{-4}
Ω_p	$(\gamma-1)\left(\frac{\rho_0}{\gamma p_0}\right)\left(\frac{\partial C}{\partial \rho}\Big\vert_p\right)_0$	1.32×10^{-4}
$\Omega_\parallel$	$(\gamma-1)\left(\frac{\kappa_\parallel T_0}{p_0 a^2}\right)$	1.45×10^{-1}
$\Omega_\perp$	$(\gamma-1)\left(\frac{\kappa_\perp T_0}{p_0 a^2}\right)$	4.83×10^{-13}
Ω_r	$\frac{\eta_0 c^2}{4\pi a^2}$	9.57×10^{-12}
Ω_J	$-(\gamma-1)\frac{d \ln \eta_0}{d \ln T_0}\frac{\eta_0 J_0^2(0)}{p_0}$	1.91×10^{-9}

$n_0 = \rho_0/m_i = 10^{10}\ \mathrm{cm}^{-3}$, $T_0 = 10^6\ K$,

$a = 100\ \mathrm{km}$, $B_0 = 83.3\ \mathrm{G}$

$\tau_h = a\sqrt{4\pi\rho_0 / B_0^2}$

Linear modes for thermal instability in a sheared magnetic field

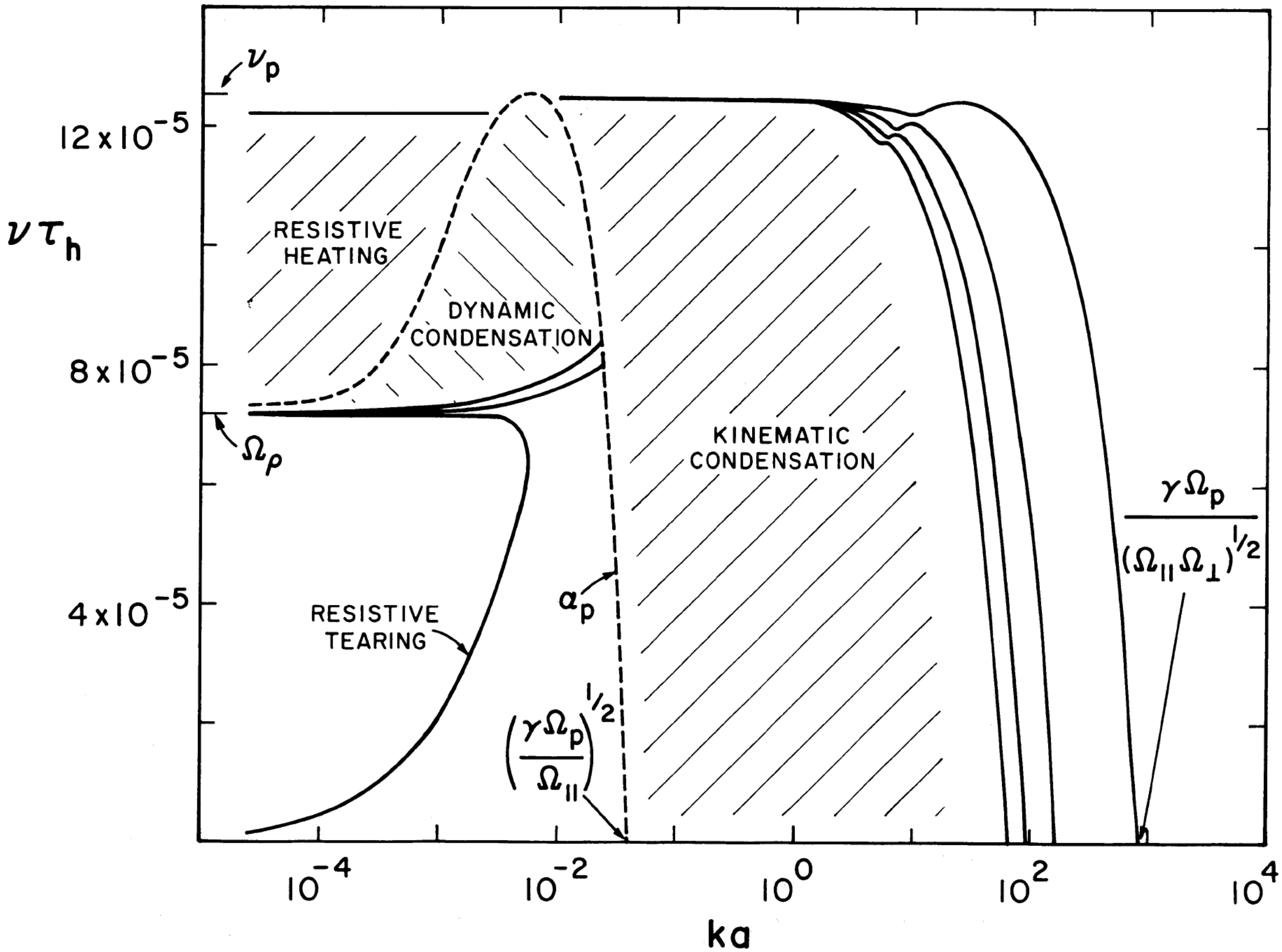

Growth rate vs. wavenumber

Dynamic condensations

Characteristics of *dynamic* condensations:

- spatial scale is determined primarily by force balance
- plasma mass flow is directed perpendicular to the magnetic field
- less compressible, the magnetic field inhibits (transverse) plasma compression
- only a drop in temperature contributes to growth
- the growth rate increases with the number of nodes in mode
- analog of classical resistive tearing mode is a special case

Density perturbations for principal dynamic condensation mode and 1st harmonic

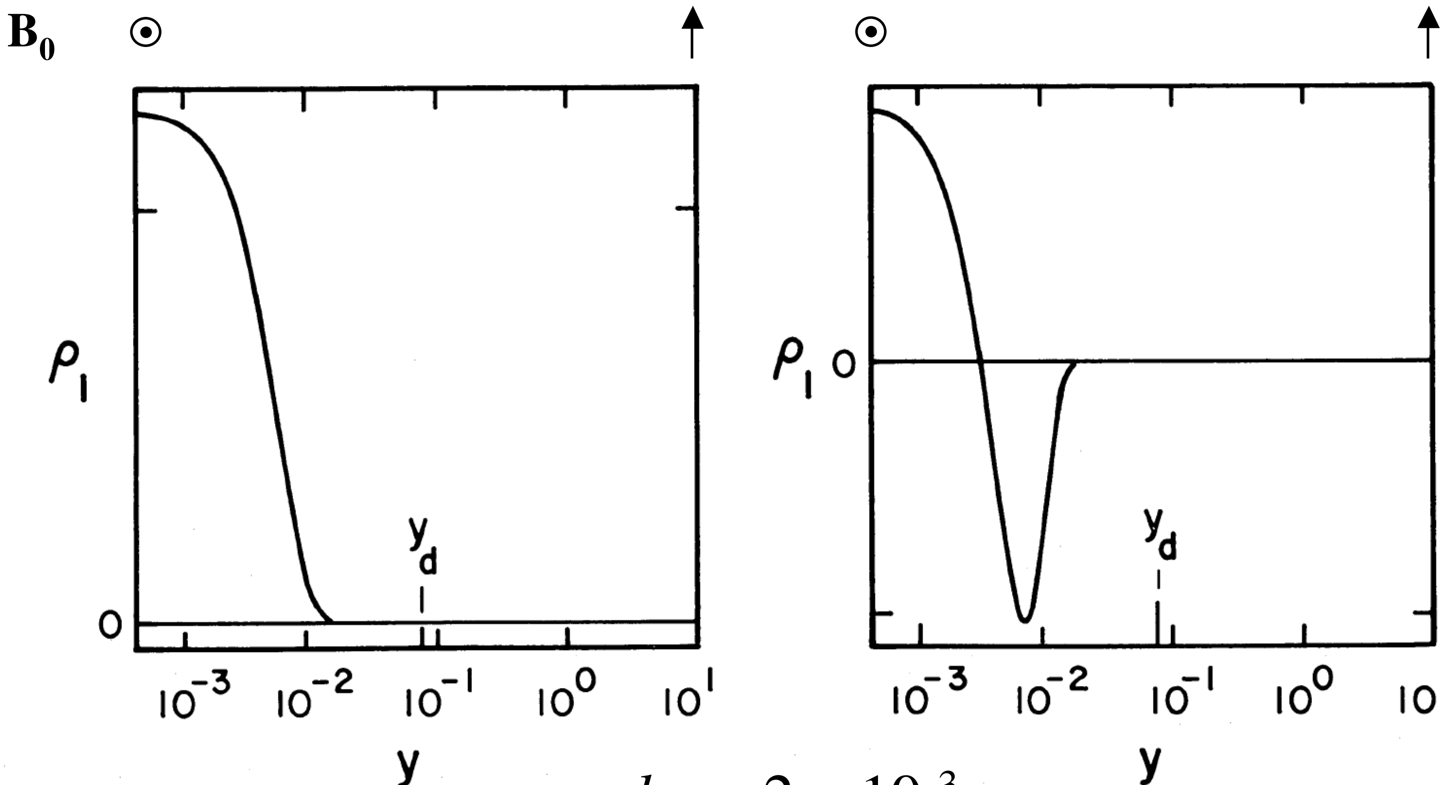

$ka = 2 \times 10^{-3}$

Characteristic spatial scale y_d defined by:

$$\frac{B_{0z}(y_d) k v_A}{B_0} = \Omega_p$$

$y << y_d$ => flow is perpendicular to $\mathbf{B_0}$.

$y >> y_d$ => flow is parallel to $\mathbf{B_0}$.

Kinematic condensations

kinematic - “of or relating to aspects of motion apart from considerations of mass and force”

Characteristics of *kinematic* condensations -

- spatial scale is determined primarily by energy balance
- exist only in the presence of anisotropic heat flow
- plasma mass flow is directed parallel to the magnetic field
- highly compressible; most compressible when sound waves traveling parallel to the magnetic field can maintain pressure balance
- both a drop in temperature and mass flow parallel to field lines contribute to growth
- exhibit higher growth rates than dynamic modes
- growth rate decreases with number of nodes in mode

Density perturbations for principal kinematic condensation mode

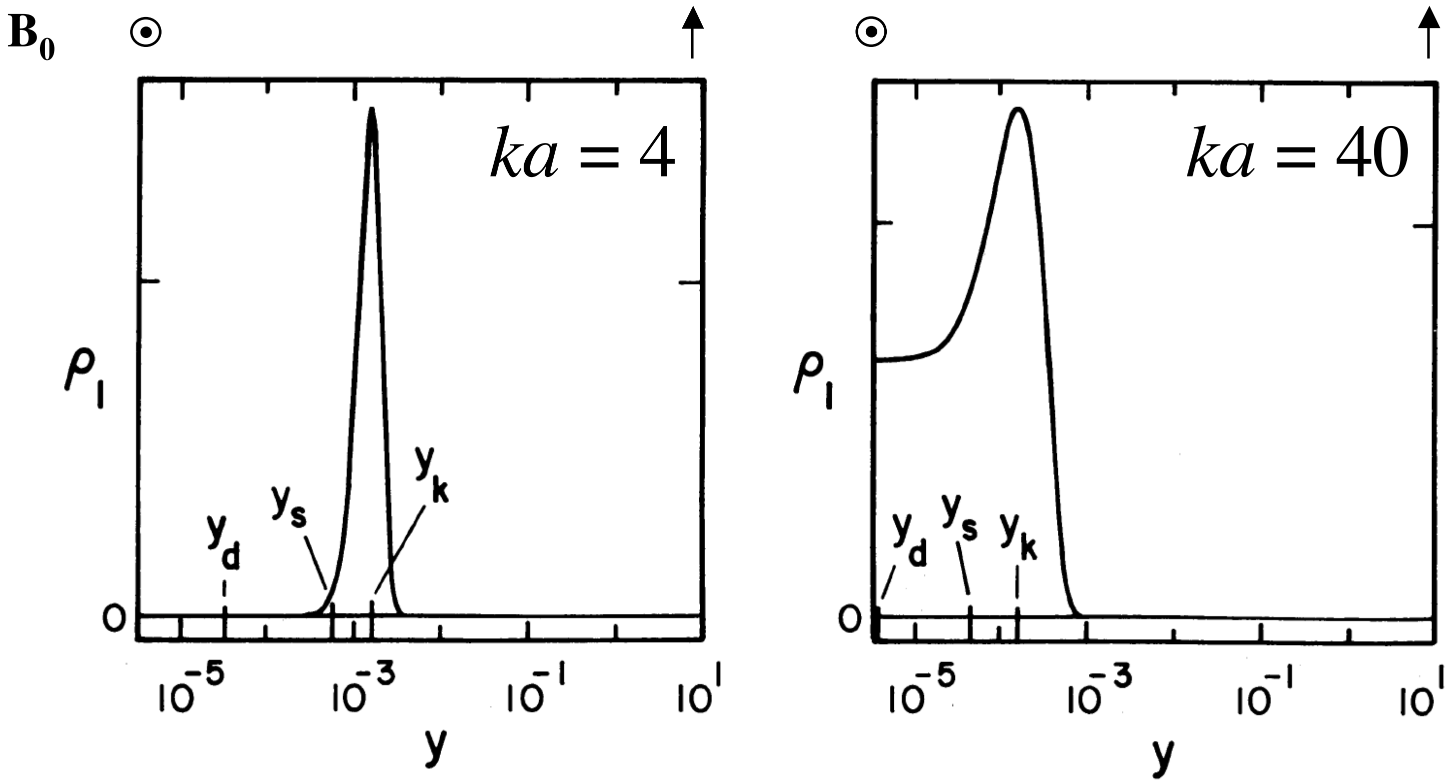

Characteristic spatial scales y_s, y_k:

$y > y_s$ => sound waves parallel to $\mathbf{B_0}$ can maintain pressure balance

$$\frac{B_{0z}^2(y_s)k^2\gamma p_0}{B_0^2\rho_0} = \upsilon^2$$

$y >> y_k$, thermal conduction dominates radiation

$$\frac{k^2 B_{0z}^2(y_k)}{B_0^2} = \frac{\gamma p_0(\Omega_p - \upsilon) - \upsilon^2\rho_0 a^2\Omega_{\|}}{2p_0 a^2\Omega_{\|}}$$

Temperature evolution for generic perturbation

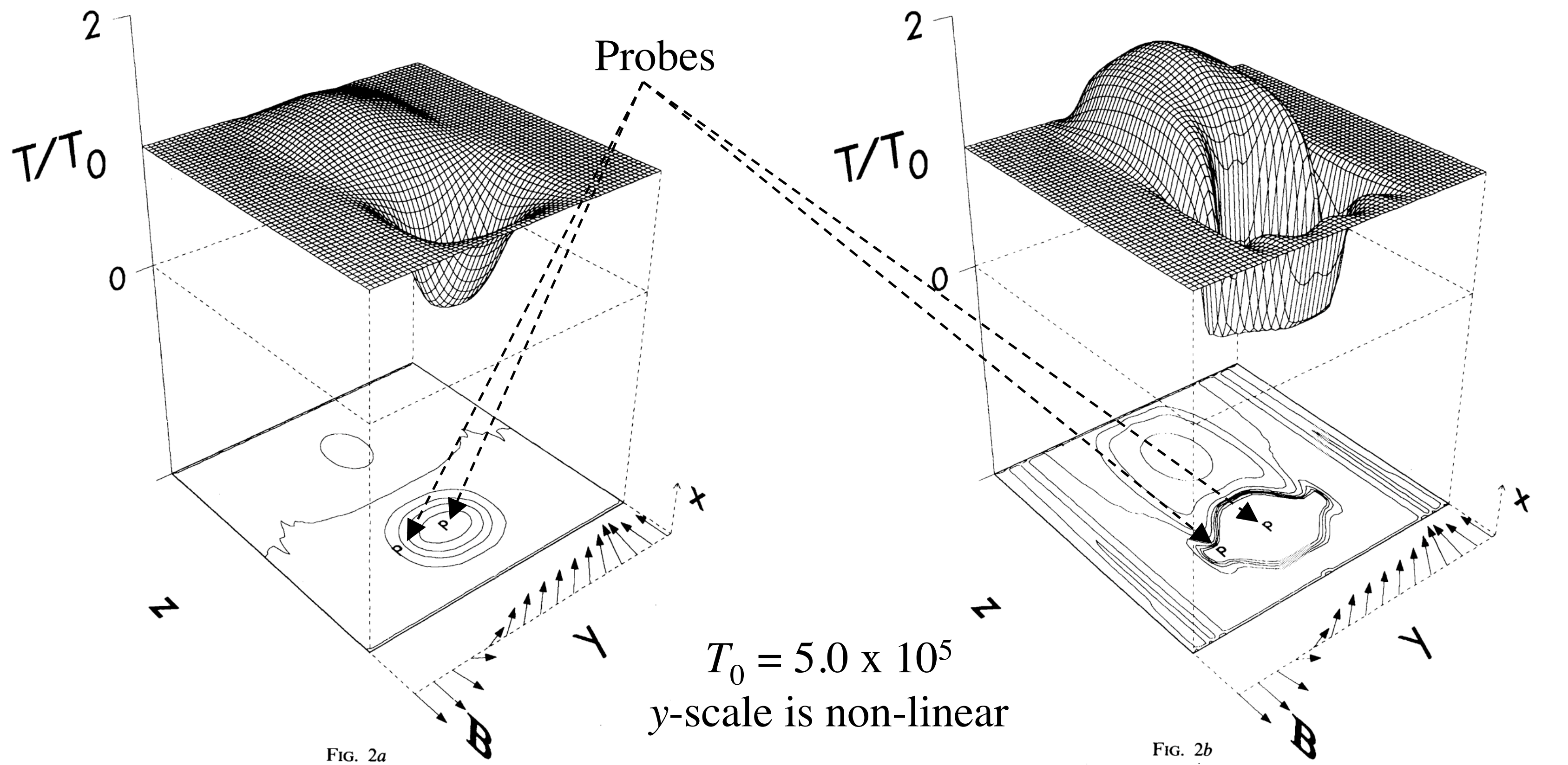

T = 178 sec

T = 293 sec

Choose **k** so that only kinematic modes are thermally unstable.

Density evolution for generic perturbation

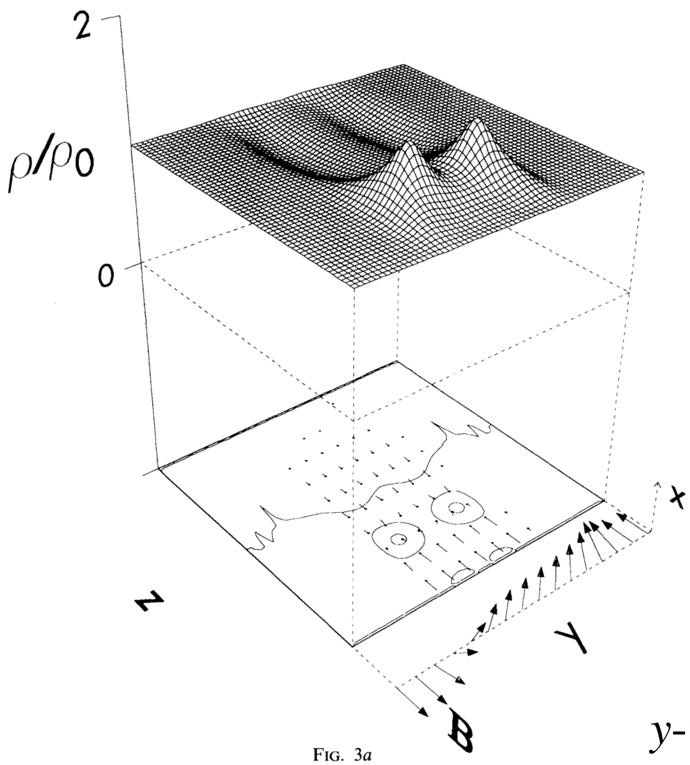

FIG. 3a

y-scale is non-linear

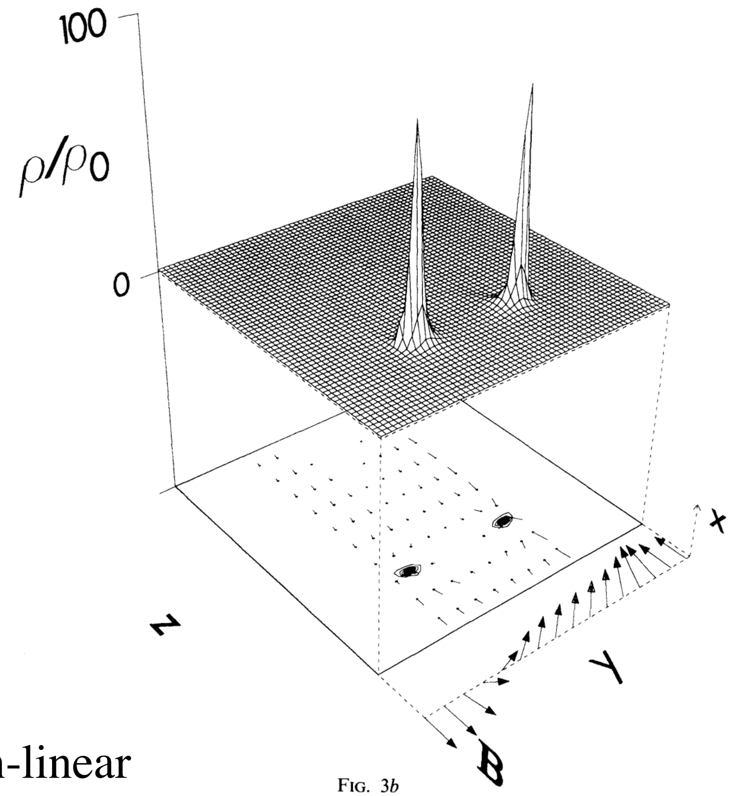

FIG. 3b

T = 178 sec

T = 293 sec

Density at peaks increases by nearly two orders of magnitude.

Time evolution at probe for generic perturbation

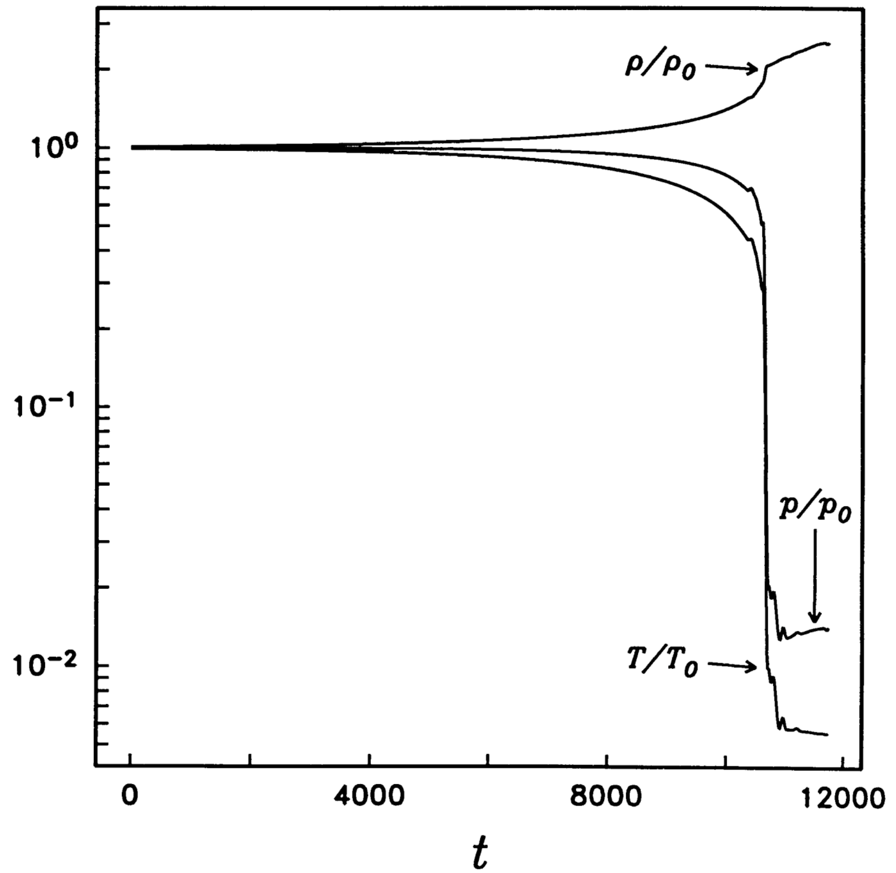

Temperature, density, and pressure

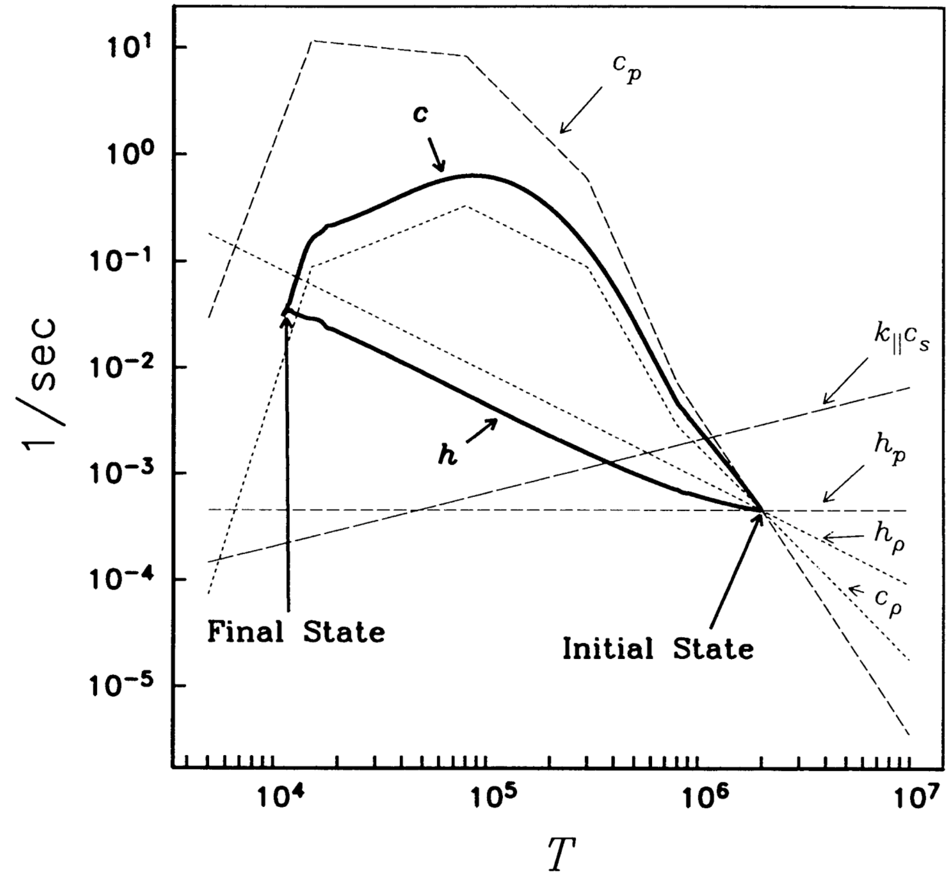

Heating rate: $h = H/p$

Cooling rate: $c = C(T)/p$

Similar results but slower to develop - a much longer computation.

Temperature evolution for random perturbation with $T_0 < T_c$

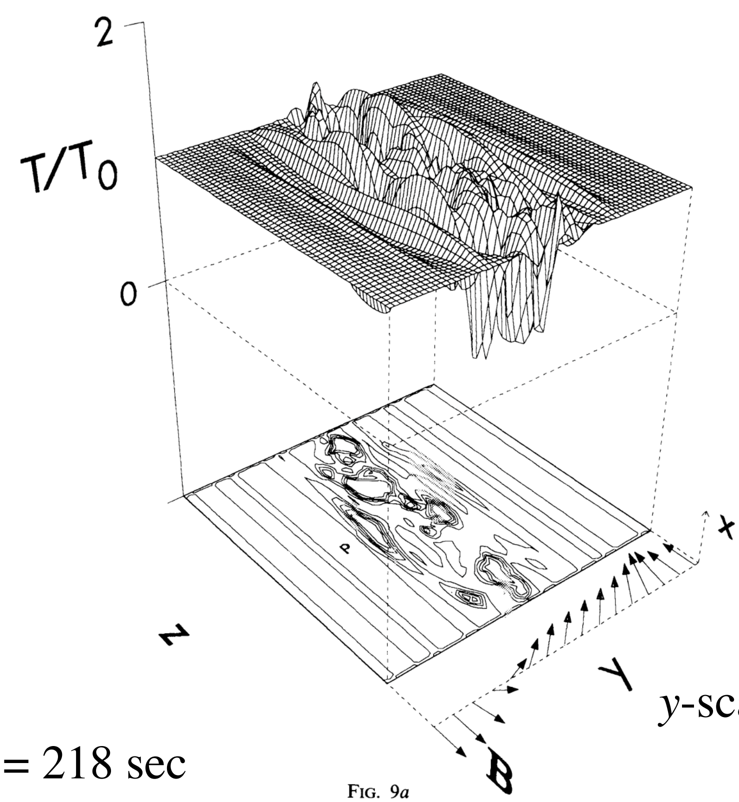

t = 218 sec

FIG. 9a

y-scale is non-linear

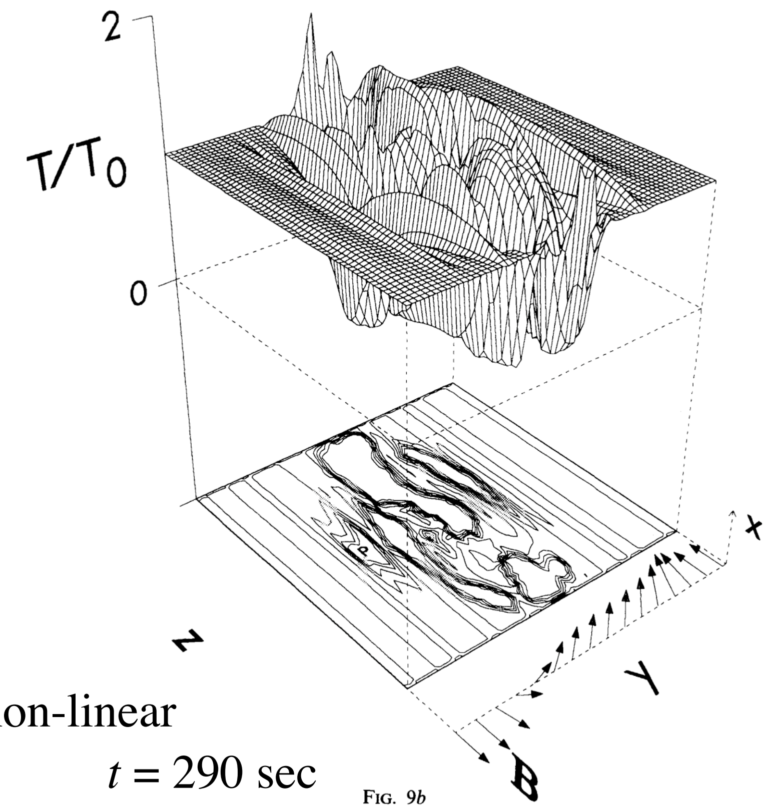

t = 290 sec

FIG. 9b

Initial temperature is $T_0 = 5 \times 10^5$ K

Final temperature in condensation is ~ T_0 / 100.

Density evolution for random perturbation with $T_0 < T_c$

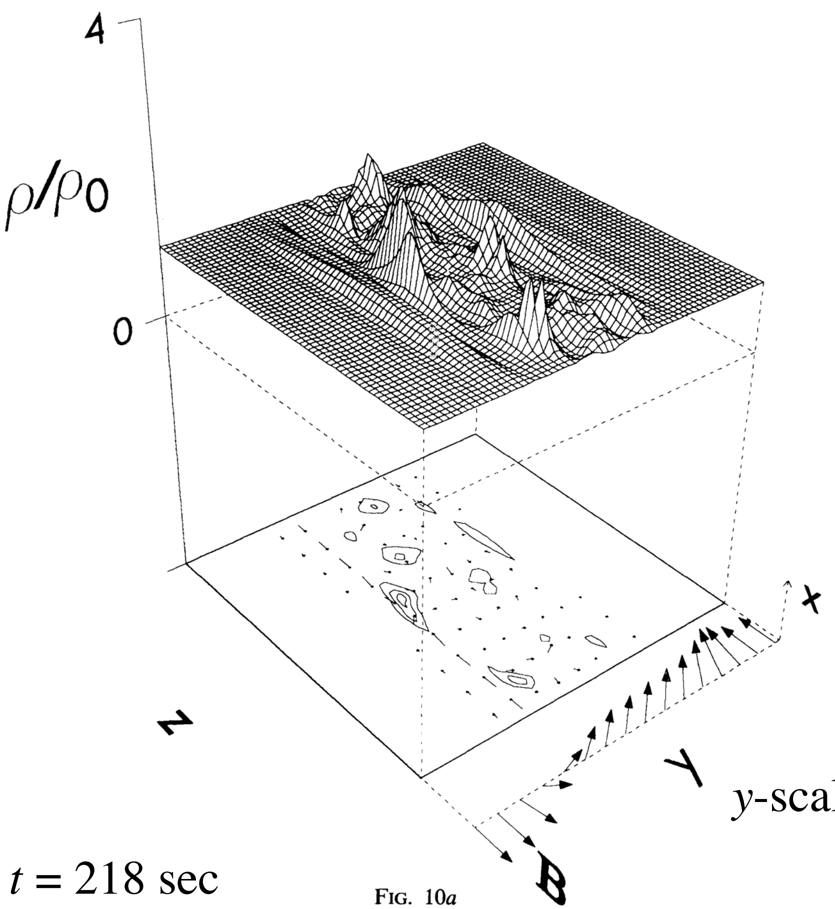

t = 218 sec

FIG. 10*a*

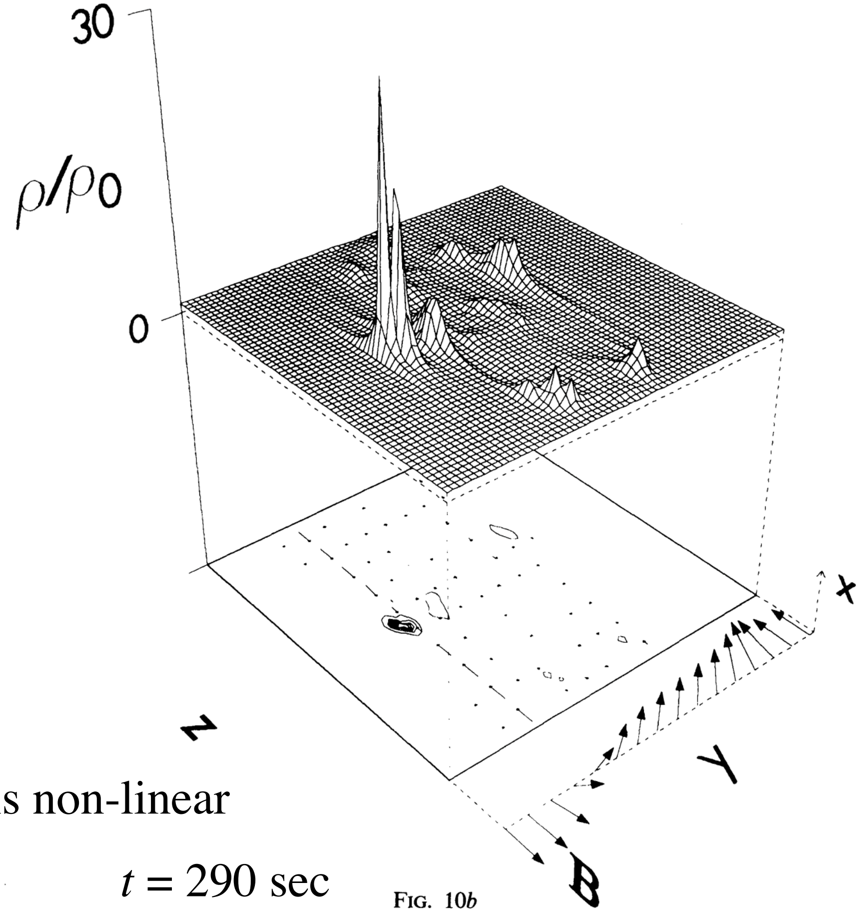

t = 290 sec

FIG. 10*b*

y-scale is non-linear

Final peak density is ~ $100\rho_0$.

Summary for linear analysis

- A condensation will form preferentially in regions near where **k** is perpendicular to $\mathbf{B_0}$.
- *Dynamic* condensations:
  - spatial structure is determined primarily by force balance;
  - have plasma mass flow perpendicular to the magnetic field;
  - growth due primarily to temperature drop.
- *Kinematic* condensations:
  - exist only in the presence of anisotropic heat flow;
  - have plasma mass flow parallel to the magnetic field;
  - are most compressible when sound waves traveling parallel to the magnetic field can maintain pressure balance;
  - both a drop in temperature and mass flow parallel to field lines contribute to growth;
  - exhibit the fastest growth.

Summary for non-linear simulations

Nonlinear two-dimensional MHD simulations have traced the local genesis and growth of plasma filament threads in a force-free, sheared magnetic field until they attain both a minimum temperature and a maximum mass density characteristic of observed solar filaments.

A locally sheared magnetic field can thermally insulate regions of a coronal plasma without simultaneously impeding the mass flow required for the growth of condensations.

Linearized equations of motion

$$\frac{1}{\rho_0}\frac{\partial \rho_1}{\partial t} + \nabla \cdot \boldsymbol{u} = 0\,,$$

$$\rho_0 \frac{\partial \boldsymbol{u}}{\partial t} + \nabla p_1 + \boldsymbol{B}_0 \times (\nabla \times \boldsymbol{B}_1)/4\pi + \boldsymbol{B}_1 \times (\nabla \times \boldsymbol{B}_0)/4\pi = 0$$

$$\frac{1}{T_0}\frac{\partial T_1}{\partial t} + (\gamma - 1)\nabla \cdot \boldsymbol{u} + \frac{(\gamma - 1)}{p_0}\left(\frac{\partial C}{\partial \rho}\,\rho_1 + \frac{\partial C}{\partial T}\,T_1\right) - \frac{(\gamma - 1)\eta_0 c^2}{8\pi^2 p_0}(\nabla \times \boldsymbol{B}_0)\cdot(\nabla \times \boldsymbol{B}_1) - \frac{(\gamma - 1)\eta_1 c^2}{16\pi^2 p_0}\,|\nabla \times \boldsymbol{B}|^2 - \frac{(\gamma - 1)}{p_0}\,\nabla \cdot \boldsymbol{\kappa}_0 \cdot \nabla T_1 = 0$$

$$\frac{\partial \boldsymbol{B}_1}{\partial t} + \frac{c^2}{4\pi}\nabla \eta_1 \times (\nabla \times \boldsymbol{B}_0) + \frac{c^2 \eta_0}{4\pi}\nabla \times (\nabla \times \boldsymbol{B}_1) - \nabla \times \boldsymbol{u} \times \boldsymbol{B}_0 = 0$$

$$\nabla \cdot \boldsymbol{B}_1 = 0\,,$$

$$\frac{p_1}{p_0} = \frac{\rho_1}{\rho_0} + \frac{T_1}{T_0}\,.$$

Linear modes in a *uniform* magnetic field

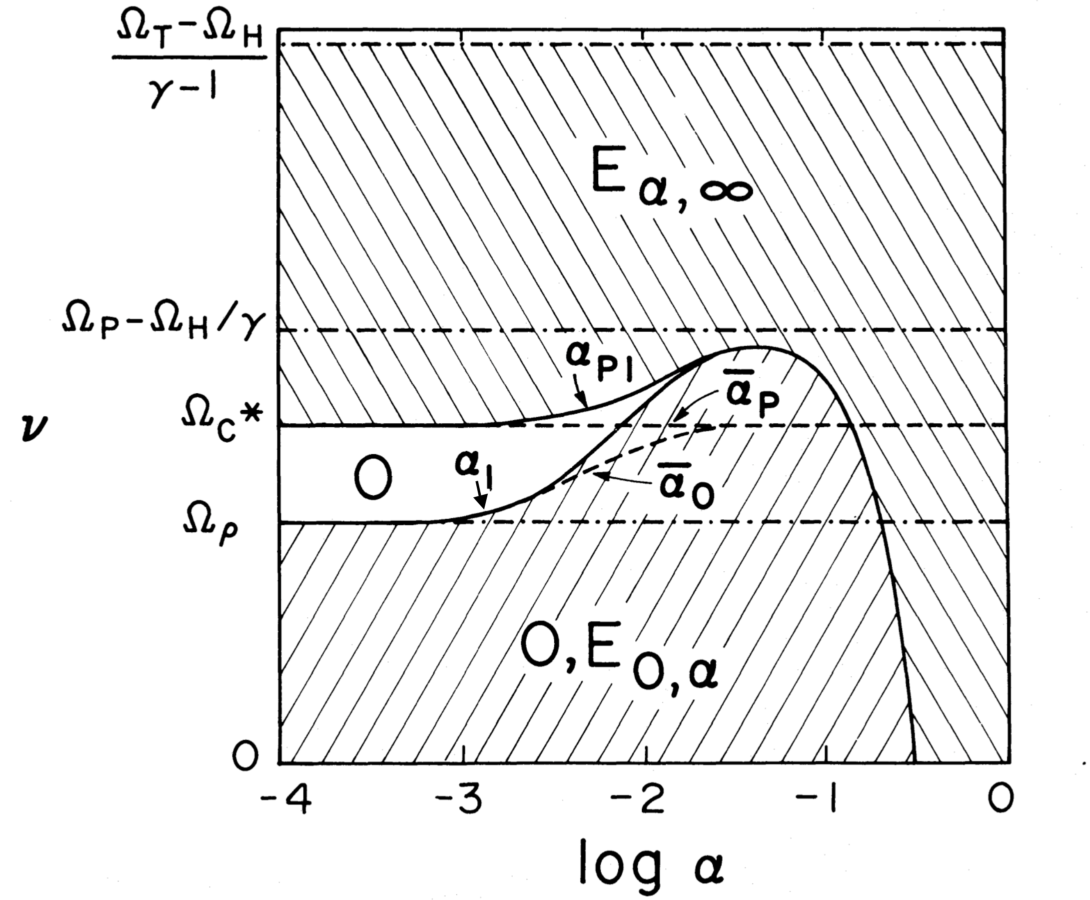

$\mathbf{k} \cdot \mathbf{B}_0 = 0$

Solutions of the form: $q(y) = (A\, e^{+sy} + Be^{-sy})\, e^{ikx}$

Growth rate vs. Lundquist number for kinematic condensation modes

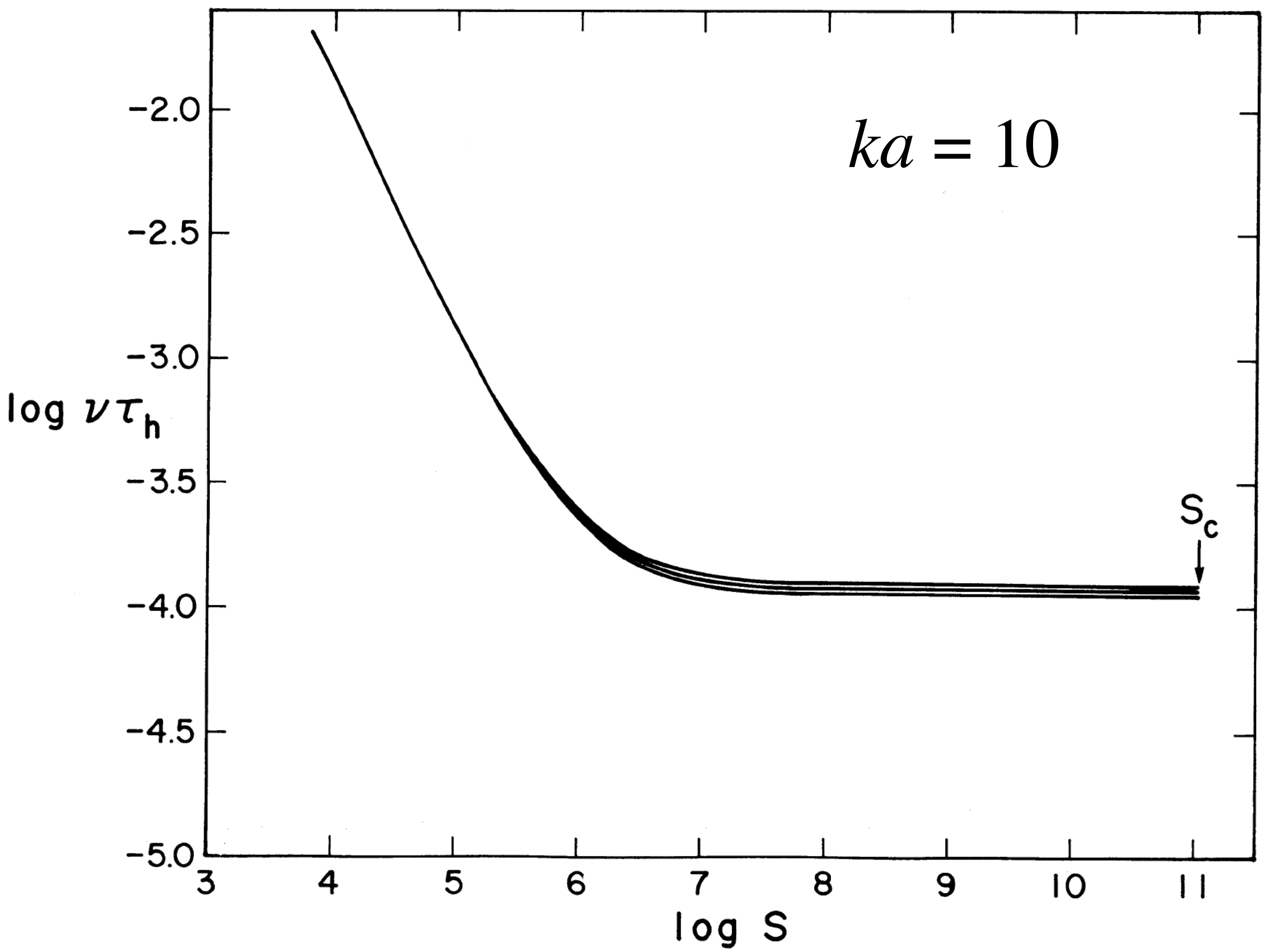

Growth rate vs. S for dynamic condensation, resistive heating mode and resistive tearing mode

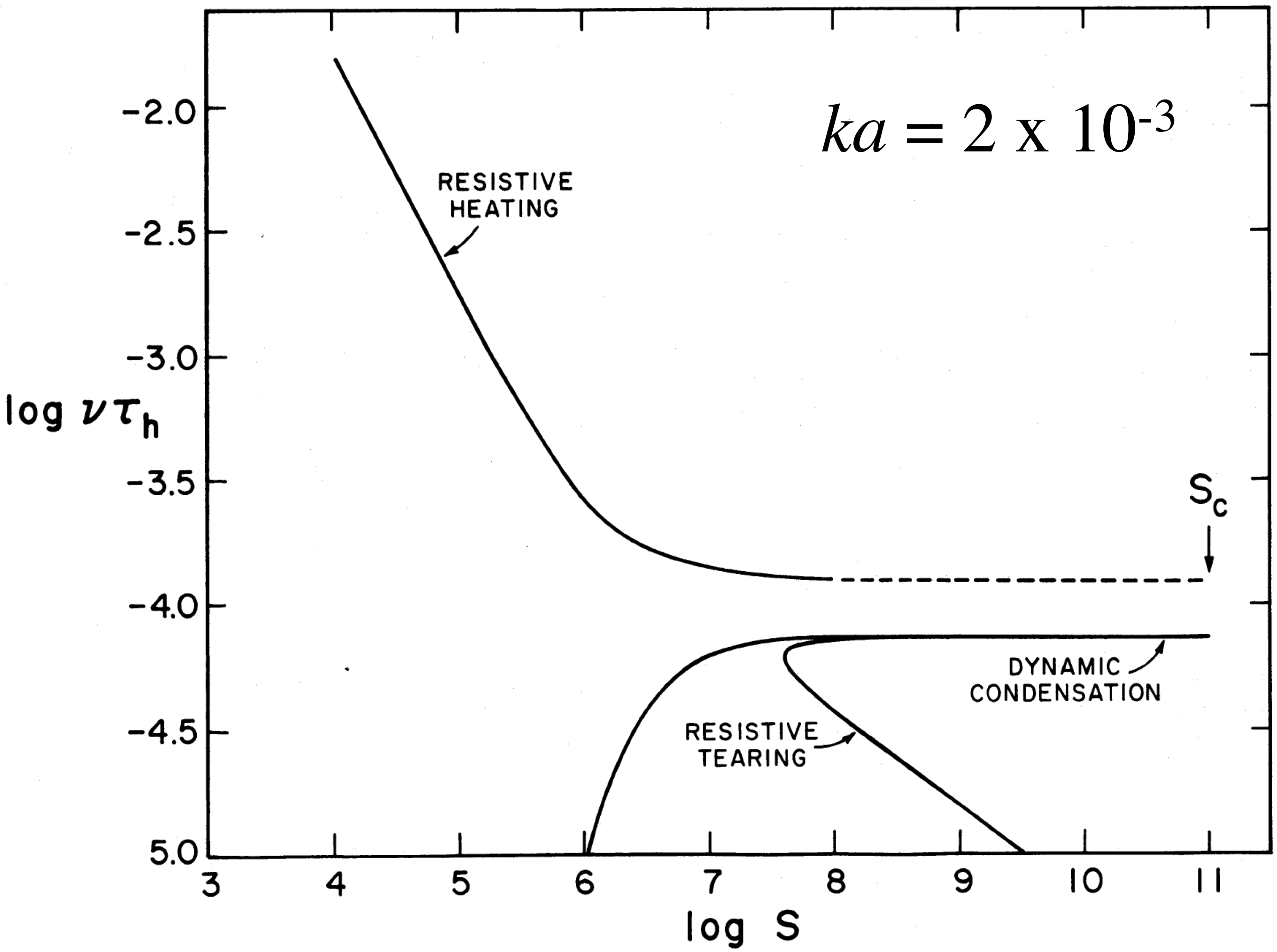

Time evolution at outer probe for generic perturbation with $T_0 < T_c$

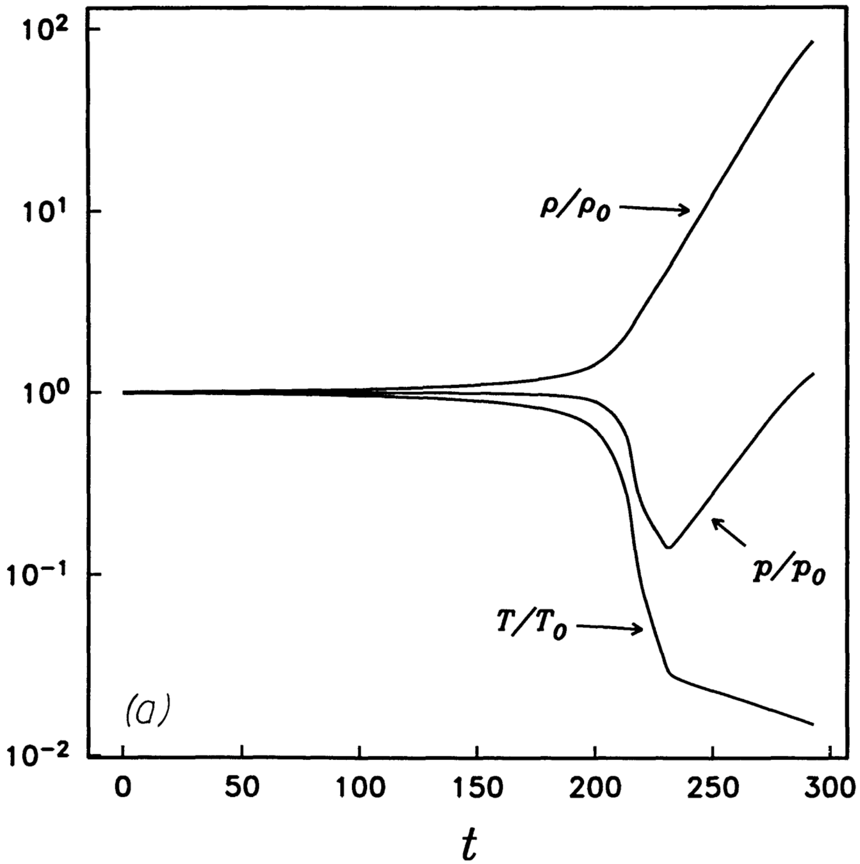

Temperature, density, and pressure

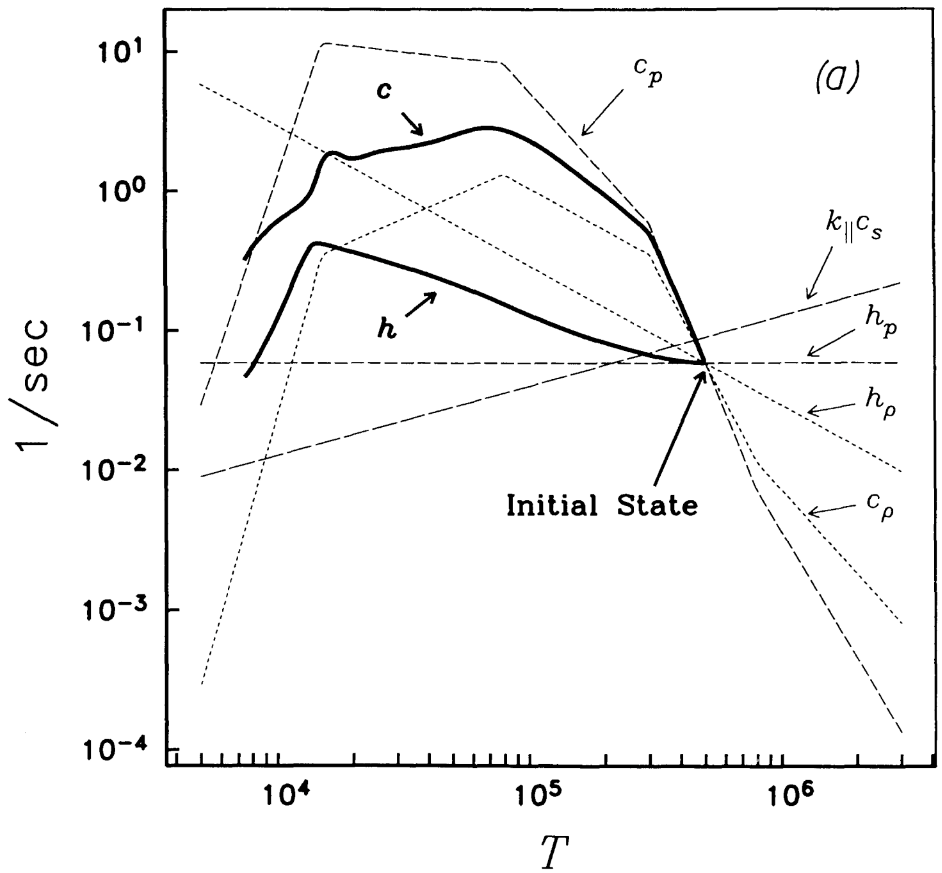

Heating rate: $h = H/p$

Cooling rate: $c = C(T)/p$

Simulation is run until gradients can no longer be resolved.

Time evolution at inner probe for generic perturbation with $T_0 < T_c$

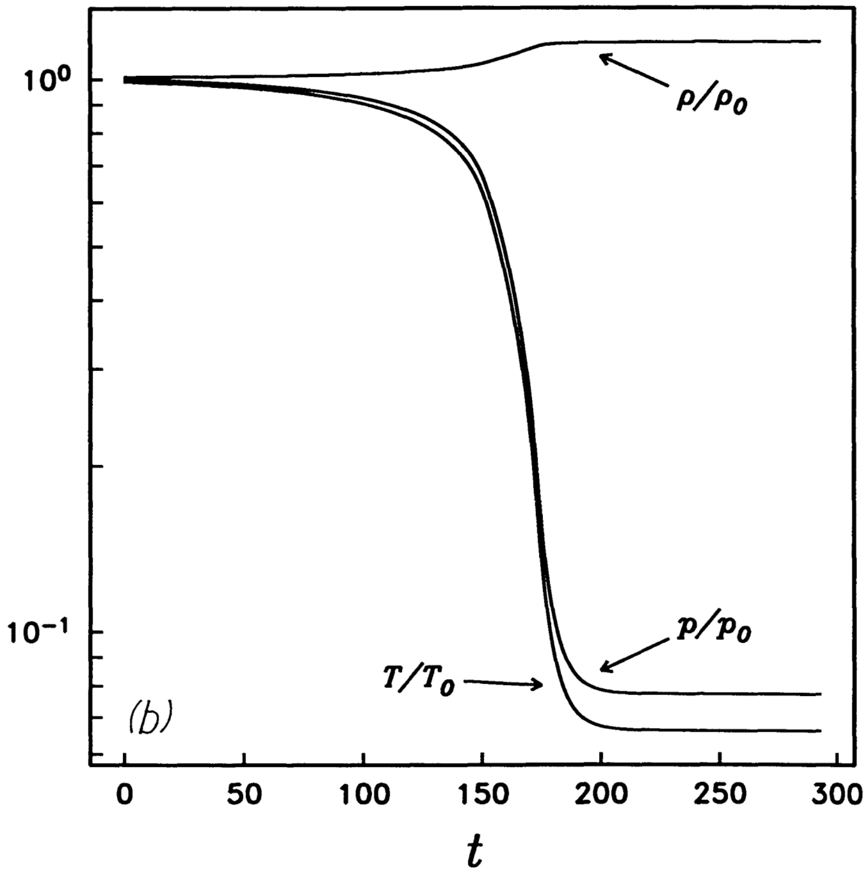

Temperature, density, and pressure

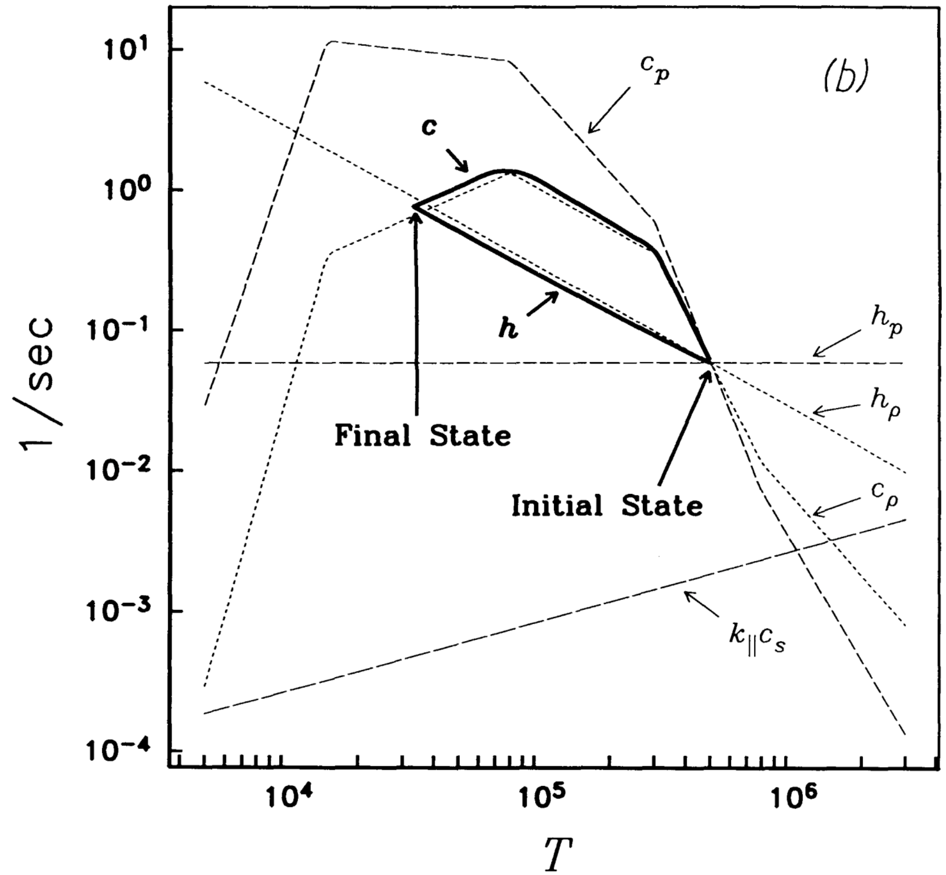

Heating rate: $h = H/p$

Cooling rate: $c = C(T)/p$

A new radiative equilibrium is established at the inner probe.

Necessary conditions for thermal instability
(Field, *Ap. J.* 142, 531, 1965)

density | temperature | pressure

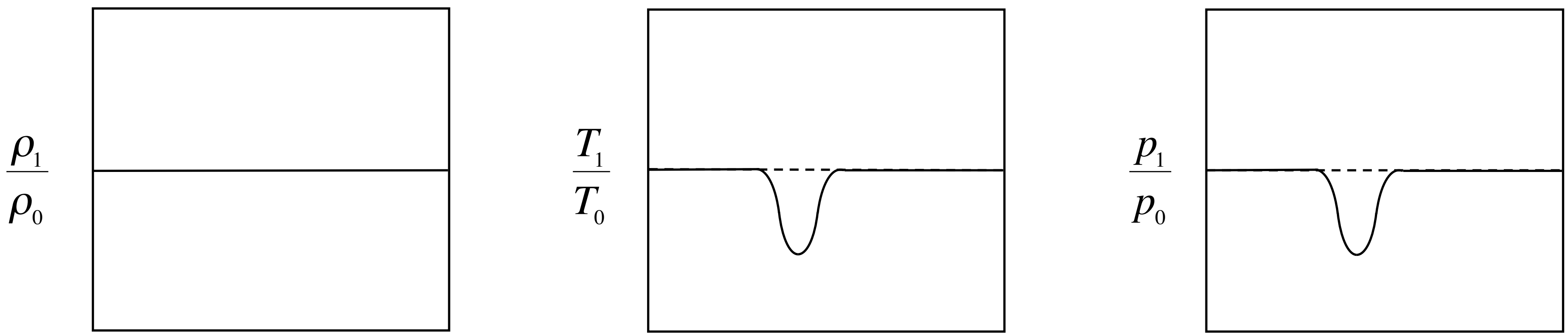

Isochoric perturbation: $\left.\frac{\partial C}{\partial T}\right|_{\rho} < 0$

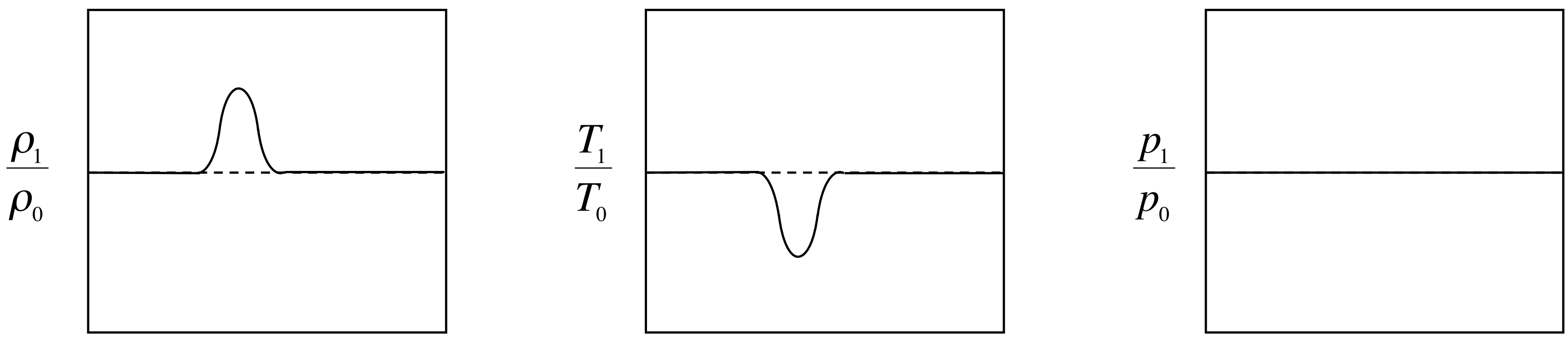

Isobaric perturbation: $\left.\frac{\partial C}{\partial T}\right|_{\rho} - \frac{\rho_0}{T_0}\left(\frac{dH}{d\rho} + \left.\frac{\partial C}{\partial \rho}\right|_{T}\right) < 0$